 CMES, vol.25, no.2, pp.69-79, 2008

Numerical Identification of the Hydraulic Conductivity of Composite Anisotropic Materials

S. D. Harris,[1] **R. Mustata**[2]**, L. Elliott**[2]**, D. B. Ingham**[2] **and D. Lesnic**[2]

Abstract: Two homogeneous anisotropic materials are butted together to form a contact surface within a single composite material (the specimen). An inverse boundary element method (BEM) is developed to determine the components of the hydraulic conductivity tensor of each material and the position of the contact surface. A steady state flow is forced through the specimen by the application of a constant pressure differential on its opposite faces. Experimental measurements (simulated) of pressure and average hydraulic flux at exposed boundaries are then used in a modified least squares functional. This functional minimises the gap between the above measured (simulated) values and their corresponding BEM values within a genetic algorithm maximisation procedure. The latter quantities are determined using the current estimates of the components of the hydraulic conductivity tensors and the position of the contact surface.

Keyword: Boundary element method, genetic algorithm, hydraulic conductivity, inverse problem.

1 Introduction

The production of gas and oil in many reservoirs is seriously affected by their highly heterogeneous and/or anisotropic structure. From the fluid flow viewpoint, it is well accepted that heterogeneity and anisotropy are two closely related properties. Non-homogeneous materials are usually thought to appear homogeneous, but anisotropic, when considered at a scale much larger than the largest scale of heterogeneity.

A number of methods have been proposed to measure the full hydraulic conductivity tensor in rocks or soils. Zhan and Yortsos (2001) identified the permeability field of an anisotropic porous medium directly from the solution of a nonlinear boundary value problem by monitoring the displacement front at successive time intervals. Fontugne (1969) performed two flow measurements simultaneously on a prepared soil, with the fluid outlets aligned with the assumed principal directions. He then determined the ratio of the principal hydraulic conductivities. The amplitudes of the principal hydraulic conductivities were measured separately. Rose (1970) designed an experimental procedure to force the streamlines to be straight lines parallel to the sample axis. However, this method required the modification by trial and error of the shape of the sample, making it difficult to implement in practice. Both of these methods assume that the sample axis can be oriented parallel or perpendicular to one of the principal directions. However, this is not as serious a restriction as it might first appear since, in many cases, at least one of the principal directions can be guessed from the bedding planes, preferred orientation of the micro-cracks, and the like. The commonly used concept of horizontal and vertical hydraulic conductivities implicitly assumes that the principal hydraulic conductivity directions insitu are likewise in orientation, but this is not always true. However, samples can be taken in directions parallel and perpendicular to the bedding planes when visible, rather than parallel and perpendicular to the axis of the core as it is usually done.

If the principal directions cannot be estimated, a different method becomes necessary. The best so-

[1] Rock Deformation Research, School of Earth Sciences, University of Leeds, Leeds, LS2 9JT, UK. email: sdh@rdr.leeds.ac.uk

[2] Department of Applied Mathematics, University of Leeds, Leeds, LS2 9JT, UK.

lution would be to measure the full hydraulic conductivity tensor in one single sample by imposing periodic boundary conditions [Durlofsky and Chung (1987); Mei and Auriault (1989); Saez, Otero, and Rusinek (1989)]. Whilst this can be achieved, it is rather difficult to implement in practice. Alternatively, it may be possible to perform a suite of independent flow measurements, each one with a different set of Neumann and Dirichlet boundary conditions. As this is perfectly possible in laboratory experiments, this method may yield enough information to allow one to infer the full hydraulic conductivity tensor. A similar idea was applied in White and Horne (1987), but in another context. Bernabe (1992) sketched a possible procedure involving six steady state flux measurements (two longitudinal and the rest diagonal) and inferred the components of the hydraulic conductivity tensor with an accuracy that varied from 10% for the largest component to 30% for the smallest.

In this paper, the steady flow of a single liquid phase through a rectangular, composite specimen, composed of two anisotropic materials with a plane contact surface, is analysed using a BEM approach. The particular geometry of the specimen has been chosen so as to correspond to the apparatus used in laboratory experiments. A genetic algorithm based inverse technique is employed for identifying the two hydraulic conductivity tensors and the contact surface position, using pressure and/or hydraulic flux values (simulated) at the exposed boundaries of the specimen.

Finally, we note that, recently, the solution of inverse problems has been undertaken numerically in a wide variety of applications in engineering and science [Shiozawa, Kubo, Sakagami, and Takagi (2006); Ling and Atluri (2006); Liu (2006); Mera, Elliott, and Ingham (2006); Liu, Liu, and Hong (2007); Huang and Shih (2007); Marin, Power, Bowtell, Sanchez, Becker, Glover, and Jones (2008)].

2 Mathematical formulation

In conventional laboratory experiments, the specimens are either rectangular blocks or cylinders. In this paper, we consider the former type of specimen which, in two-dimensions, can be represented as a rectangle. The specimen under investigation consists of two materials which we label as sample X and sample Y. A steady state flow situation exists in which the fluid is forced through the specimen by applying the constant pressures $\overline{p} = \overline{p}_0$ and $\overline{p} = \overline{p}_0 - \delta\overline{p}_0$, where $\delta\overline{p}_0 > 0$, on opposite faces. The equation describing the conservation of mass can be combined with the generalised form of Darcy's law for anisotropic materials to give the equation of single-phase incompressible fluid flow in a two-dimensional, composite porous material within the rectangular domain Ω. In non-dimensional form, assuming that the total length of the specimen has the non-dimensional value $L = 2$, the governing equation can then be written in the reference frame (x,y) as

$$k_{11}\frac{\partial^2 p}{\partial x^2} + 2k_{12}\frac{\partial^2 p}{\partial x \partial y} + k_{22}\frac{\partial^2 p}{\partial y^2} = 0\,, \tag{1}$$

for $(x,y) \in \Omega = (0,2) \times (0,1)$, where k_{ij} denote the components of the constant hydraulic conductivity tensor $\boldsymbol{k}$, with $k_{11}k_{22} > k_{12}^2$, and $p = (\overline{p} - (\overline{p}_0 - \delta\overline{p}_0))/\delta\overline{p}_0$ is the non-dimensional pressure. In the same reference frame, the boundary conditions corresponding to the application of the pressure differential between the faces $x = 0$ (inflow) and $x = 2$ (outflow), with sealed top ($y = 1$) and bottom ($y = 0$) boundaries, can be written as

$$\begin{aligned} &p|_{x=0} = 1, \quad p|_{x=2} = 0, \\ &\left.\frac{\partial p}{\partial \nu^+}\right|_{y=0} = \left.\frac{\partial p}{\partial \nu^+}\right|_{y=1} = 0\,, \end{aligned} \tag{2}$$

where

$$\frac{\partial}{\partial \nu^+} = \sum_{i,j=1}^{2} k_{ij}\cos(\nu^+, x_i)\frac{\partial}{\partial x_j} \tag{3}$$

with the convention that $x_1 = x$, $x_2 = y$ and $\cos(\nu^+, x_i)$ are the direction cosines of the positive normal ν^+ to the surface of the sample. Figure 1 shows that the contact surface between sample X and sample Y is defined by distances x_b^f and x_t^f measured from the inflow face of the specimen along the bottom ($y = 0$) and top ($y = 1$) no-flow boundaries, respectively. This contact surface is

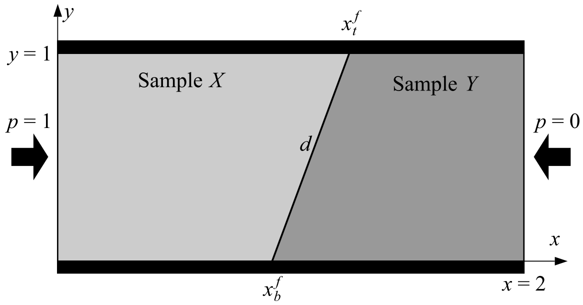

Figure 1: Configuration considered in the mathematical model of the problem.

considered to provide discontinuities in the hydraulic conductivity tensor components.

At the plane contact surface d, defined by

$$d=\left\{(x,y):y=\frac{x-x_b^f}{x_t^f-x_b^f},\ x_b^f\leqslant x\leqslant x_t^f\right\}, \tag{4}$$

the pressure and hydraulic flux are assumed to be continuous functions, i.e.

$$\begin{aligned}\lim_{(x,y)\in X\nearrow d} p &= \lim_{(x,y)\in Y\searrow d} p\,,\\ \lim_{(x,y)\in X\nearrow d}\frac{\partial p}{\partial \nu^+} &= \lim_{(x,y)\in Y\searrow d}\frac{\partial p}{\partial \nu^+}\,.\end{aligned} \tag{5}$$

Each of the homogeneous anisotropic materials has a constant hydraulic conductivity tensor defined by

$$\boldsymbol{k}^{\mathrm{s}}=\begin{pmatrix}k_{11}^{\mathrm{s}} & k_{12}^{\mathrm{s}}\\ k_{12}^{\mathrm{s}} & k_{22}^{\mathrm{s}}\end{pmatrix},$$

where the superscript $\mathrm{s}\in\{X,Y\}$. However, a better insight into the physics of the problem is provided by a set of related quantities. Therefore, we provide, and look for, values of the principal hydraulic conductivities, k_1^{s} and k_2^{s}. We assume that $k_1^{\mathrm{s}}>k_2^{\mathrm{s}}$ and that the direction of k_1^{s} for each material makes an angle θ^{s} with the x-axis. In the (x,y) coordinate system, the components of the hydraulic conductivity tensors are given by the following relations:

$$\begin{aligned}k_{11}^{\mathrm{s}}&=k_1^{\mathrm{s}}\cos^2\theta^{\mathrm{s}}+k_2^{\mathrm{s}}\sin^2\theta^{\mathrm{s}}\,,\\ k_{12}^{\mathrm{s}}&=(k_1^{\mathrm{s}}-k_2^{\mathrm{s}})\cos\theta^{\mathrm{s}}\sin\theta^{\mathrm{s}}\,,\\ k_{22}^{\mathrm{s}}&=k_2^{\mathrm{s}}\cos^2\theta^{\mathrm{s}}+k_1^{\mathrm{s}}\sin^2\theta^{\mathrm{s}}\,,\end{aligned} \tag{6}$$

where $\theta^{\mathrm{s}}\in\left\{\theta^X,\theta^Y\right\}$ can be different from one sample to another.

We consider two situations concerning the contact surface orientation. In the first, the contact surface is assumed perpendicular to the x-axis of the sample, namely $x_t^f=x_b^f$. In the second, the contact surface is inclined to the x-axis, namely $x_t^f\neq x_b^f$.

3 The direct problem

This section addresses the boundary discretization adopted to solve the direct, well-posed problem, as defined by Eq. (1), and the boundary and interface conditions (2) and (5).

The bottom and top no-flow boundaries of the specimen are each divided into M equally-sized intervals $[x_{b,i-1},x_{b,i}]$ and $[x_{t,i-1},x_{t,i}]$, respectively, for $i=\overline{1,M}$, with $x_{b,0}=x_{t,0}=0$ and $x_{b,M}=x_{t,M}=2$. Depending on the values of x_b^f and x_t^f, we determine to which of the intervals from the discretization of the boundary the contact surface belongs. Let $W_b<M$ and $W_t<M$ denote the elements on the bottom and top boundaries, respectively, in which the contact surface is situated, i.e. $x_{b,W_b-1}<x_b^f<x_{b,W_b}$ and $x_{t,W_t-1}<x_t^f<x_{t,W_t}$. Then on the bottom and the top no-flow boundaries of sample X we have a total of W_b+W_t-2 elements of length $2/M$ and two special elements of length $x_b^f-2\,(W_b-1)/M$ and $x_t^f-2\,(W_t-1)/M$. Accordingly, the bottom and the top no-flow faces of sample Y are discretized into $2M-W_b-W_t$ elements of length $2/M$ and two special elements of length $2W_b/M-x_b^f$ and $2W_t/M-x_t^f$. The inflow and outflow faces of the specimen and the contact surface are each discretized into N elements, and these elements have sizes $1/N$ and $\left(\sqrt{\left(x_b^f-x_t^f\right)^2+1}\right)/N$, respectively. These sets of elements are equal in size only when $x_b^f=x_t^f$. If x_b^f or x_t^f coincides with one of the extremities of the interval, namely x_{b,W_b-1}, x_{b,W_b}, x_{t,W_t-1} or x_{t,W_t}, then we require only elements of length $2/M$ on either the bottom or top face of the composite material. Over each element created in such a manner, the pressure function p, as well as its normal derivative, are assumed to be constant and take their values at the mid-point of the element.

To our problem we apply a classical BEM formulation [Brebbia, Telles, and Wrobel (1984)]. The resulting linear system of equations includes as unknowns the following:

- the pressure on the bottom and top boundaries;
- the hydraulic flux at the inflow and outflow faces of the specimen; and
- the pressure and hydraulic flux at the contact surface determined by Eq. (4).

The two cases studied were as follows:

(a) When the contact surface is perpendicular to the x-axis of the specimen, namely $x_t^f = x_b^f$, we consider that sample X has a non-dimensional length of $L_1 = 1.33$ and the magnitudes of the principal hydraulic conductivities are given by $k_1^X = 5$, $k_2^X = 1$, with $\theta^X = 30°$ being the angle that the x-axis of the specimen makes with the direction of k_1^X. The sample Y has a non-dimensional length of $L_2 = L - L_1 = 0.67$ and the hydraulic properties are defined by the values $k_1^Y = 5$, $k_2^Y = 1$ and $\theta^Y = 60°$.

(b) When the contact surface is inclined to the x-axis of the specimen, namely $x_t^f \neq x_b^f$, whilst the hydraulic properties and the non-dimensional length of the specimen remain as in (i), the parameters defining the contact surface are chosen to be $x_t^f = 1.42$ and $x_b^f = 1.23$.

Comparisons of the pressure distribution within the specimen for numerical simulations with $N \in \{5, 10, 20\}$ and $M = 2N$ were carried out. As demonstrated in Fig. 2 for case (a), the pressure distribution along the bottom no-flow face of the specimen becomes graphically indistinguishable for values of $N \geqslant 10$. Therefore, we do not present results for $N = 20$. As the choice $N = 10$, $M = 20$ produces a sufficiently accurate numerical solution to the direct problem, we use this grid in the numerical inversion presented next.

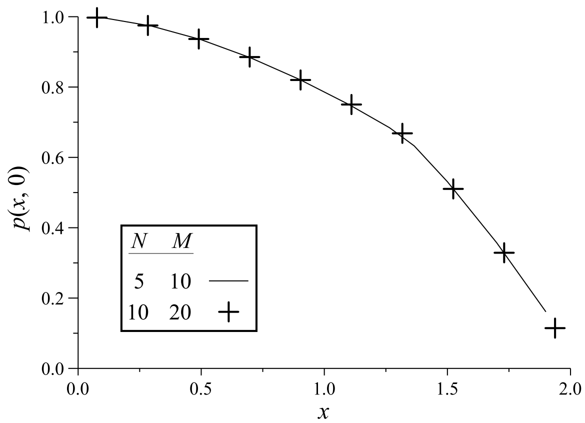

Figure 2: Numerically simulated pressure distribution along the bottom no-flow boundary of the butted sample for several grid sizes.

4 Inverse numerical formulation

The inverse analysis involves identifying values of:

- the principal hydraulic conductivities, k_1^s and k_2^s;
- the angles, θ^s, between the directions of k_1^s and the horizontal (x-axis) of the specimen; and
- the parameter values that determine the contact surface, namely x_t^f and x_b^f.

We use genetic algorithm (GA) optimisation to determine the best set of these parameters. Minimal data inputs to the GA include local measurements of the pressure and/or average hydraulic flux on the boundary of the specimen. Therefore, in practice, possible required measurements include pressure readings at ports situated on the bottom and top no-flow boundaries and average flux values taken at either end of the sample (in the steady state regime these average fluxes have the same absolute value).

Pressure alone is inadequate for accurately determining the hydraulic parameters because many parameter sets match these measurements. This non-uniqueness is most easily demonstrated by dividing Eq. (1) by one of the components of the hydraulic conductivity tensor. The result is an equivalent problem that depends only upon the ratios of these parameters rather than their individual values. The non-uniqueness of the retrieved original parameters can be overcome if one also measures non-zero average hydraulic flux values in the inversion process. In that case one must pay particular attention to the use of an effective combination of pressures and fluxes, mainly due to their different magnitudes. Therefore, we define the modified least squares objective function

$$\mathrm{LS} = \left[\alpha + \sum_{j=1}^{N_T} \frac{1}{\alpha_{T_j}} \left[(T_j)^{\mathrm{calc}} - (T_j)^{\mathrm{orig}}\right]^2\right]^{-1}, \quad (7)$$

where the superscripts (calc) and (orig) denote the BEM numerically predicted and the simulated (or measured) data values, respectively, and we record N_T data measurements T_j that can denote a pressure or an average hydraulic flux value. Furthermore, for each $j = \overline{1, N_T}$, the normalising factor α_{T_j} is chosen as a representative value of the measurement T_j to ensure a valid comparison between quantities of different orders of magnitude. The constant $\alpha = 10^{-8}$ was chosen to be small enough so that significant errors in the sums of the squared differences are always sufficiently larger than α. The GA-based optimisation technique is employed to search in an *a priori* specified range for each of the unknown parameters. The LS functional (7) which is maximised then indicates the 'fitness' of each parameter set based upon the constraints provided by the simulated or measured data values.

The GA process for identifying the unknown parameters begins by randomly constructing an initial population of N_{pop} chromosomes, each of which characterises estimates to the solution of the problem through their separate genes. The genes represent encodings of the unknown parameters over specified ranges. We employ k-tournament selection, with associated probability p_T, and a fitness evaluation function, as given by (7), which measures the accuracy of the predicted pressure and/or hydraulic flux values against some known (simulated or experimental) measurements. From the simplest procedures available, two-point crossover, with associated probability p_c, and bit-by-bit mutation, with associated probability p_m, are used to derive child chromosomes and form a pool of offspring of size N_{child}. However, alternative and more complex chromosome processing operators could have been employed. Using an elitist approach, the n_e fittest individuals from the parent population are retained for the next generation. These steps are repeated either for a specified number of generations or until a match to the imposed data is achieved to within a desired tolerance.

There are only very general guidelines as to how to choose the values of the GA evolution parameters. The typical values $N_{\mathrm{pop}} = 50$, $N_{\mathrm{child}} = 60$, $p_m = 0.02$, $p_c = 0.65$, tournament pool size $k = 2$, $p_T = 0.8$ and $n_e = 2$, which are maintained throughout this study, have been chosen based upon the numerical experiments reported by the authors for related inverse problems [Mustata, Harris, Elliott, Ingham, and Lesnic (1999); Mustata, Harris, Elliott, Lesnic, Ingham, Khachfe, and Jarny (2001)]. The domain in which the GA does its search is highlighted for each of the individual cases studied.

5 Numerical results and discussion

5.1 Contact surface perpendicular to x-axis of sample: $x_t^f = x_b^f$ (case (a))

For inversion purposes, information is provided by pressure readings at ports situated on the bottom and top no-flow boundaries of the butted sample, with the aim of employing a minimal number of ports to ensure that the required parameters are successfully retrieved.

First, we consider the configuration 'XY' in which the sample X of length $L_1 = 1.33$ is situated at the inflow face (on which $p = 1$) and we locate ports P_1 and P_2, which provide pressure measurements, at distances $x_{P_1} = 0.35$ and $x_{P_2} = 1.65$ on the bottom boundary, respectively. If we assume that the hydraulic properties of both X and Y are known, a first investigation is made into the possible retrieval of the contact surface position $x_t^f = x_b^f = 1.33$ when using just pressure readings at these ports. The range in which the search takes place is defined by $x_b^f \in \mathscr{D} = [0.5, 1.5]$ and a successful retrieval of the contact surface position is possible only if we utilise measurements situated in both samples. For example, if pressure is recorded at P_1 and P_2, a typical stable retrieved value for the contact surface position is $x_t^f = x_b^f = 1.33$, to two decimal places. This means that for the whole inversion process we will require at least one boundary pressure reading from each of the two samples.

However, as we established before, pressure alone does not provide sufficient information for retrieving the unknown hydraulic properties of the sample. Therefore, in the following calculations we add to the inversion information the average hydraulic flux value measured at the inflow face. In order to ensure a valid combination of these two types of information we perform a sensitivity analysis. Having experimented with pressure measurements from other ports on the no-flow boundaries of the samples, we reached the conclusion that the average hydraulic flux is approximately ten times more sensitive to changes in the sample parameters than is any pressure measurement at the ports. Therefore, in order to perform an effective GA search, using both pressure and average hydraulic flux information in the expression of the fitness function, we have to scale accordingly the term containing the latter contribution.

The complete inversion process provides estimates for the hydraulic conductivity parameters, k_1^s, k_2^s and θ^s in each sample, and the contact surface location, $x_b^f = x_t^f$. We begin the inversion process with an underspecified situation, namely pressure measurements from the two ports on both no-flow faces of the sample, and the average flux value measured at the inflow. Pressure ports are located at the coordinate points $(0.35,0)$, $(0.35,1)$ and $(1.65,0)$, $(1.65,1)$. These give five measurements (four pressures and average flux) with seven parameters to be identified. The following ranges are prescribed:

$$\left(\left(k_1^X,k_2^X,\theta^X\right),\left(k_1^Y,k_2^Y,\theta^Y\right),x_b^f=x_t^f\right)\in\mathscr{D}$$
$$=\Big(([4.5,5.5]\times[0.5,1.5]\times[20^\circ,40^\circ]),$$
$$([4.5,5.5]\times[0.5,1.5]\times[50^\circ,70^\circ]),([0.5,1.5])\Big),$$

and these ensure a significant pressure variation within the sample. The results of several runs, such as the ones presented as Run1 and Run2 in Tab. 1, suggest that the lack of information may not be overcome by the numerical optimisation scheme, thus resulting in the non-uniqueness of the solution. A detailed study concerning these results, by means of a comparison with a traditional numerical optimisation scheme, will be undertaken in Section 6.

Table 1: Numerical results for the GA simultaneous recovery of the principal hydraulic conductivities, k_1^s and k_2^s, the angles, θ^s, and the contact surface position in the underspecified situation.

		Run1		Run2	
Coefficient	Exact	Range	Results	Range	Results
k_1^X	5	$[4.5,5.5]$	5.06	$[4.5,5.5]$	5.19
k_2^X	1	$[0.5,1.5]$	1.02	$[0.5,1.5]$	1.04
θ^X	30°	$[20^\circ,40^\circ]$	30.46	$[20^\circ,40^\circ]$	31.02
k_1^Y	5	$[4.5,5.5]$	4.54	$[4.5,5.5]$	4.77
k_2^Y	1	$[0.5,1.5]$	0.99	$[0.5,1.5]$	1.00
θ^Y	60°	$[50^\circ,70^\circ]$	58.35	$[50^\circ,70^\circ]$	59.06
$x_b^f=x_t^f$	1.33	$[0.5,1.5]$	1.32	$[1.0,1.4]$	1.33

Due to the above non-uniqueness, we propose to move towards a fully specified situation and to investigate the accurate retrieval of the unknown parameters. A first successful attempt is one in which three pressure measurements recorded in each sample, coupled with the average inflow flux value, provides seven items of information for retrieving seven unknowns. Pressure measurements are taken at ports having coordinate positions $(0.35,0)$, $(0.65,0)$, $(1.55,0)$, $(1.85,0)$ on the bottom no-flow face and $(0.55,1)$, $(1.75,1)$ on the top no-flow face. Typical retrieved values, using the same ranges as considered in Run2 of Tab. 1, were accurate to within 1%, namely $\left(k_1^X,k_2^X,\theta^X\right)=(5.02,1.00,29.97)$, $\left(k_1^Y,k_2^Y,\theta^Y\right)=(4.98,1.00,59.98)$ and $x_b^f=x_t^f=1.33$. The error in the retrievals did not increase for larger parameter ranges, suggesting that the GA optimisation scheme produces results that are close to the optimal ones when considering the above information in the inversion process.

Another technique is to perform the inversion in a sequence of steps. In the first two steps, by interchanging the positions of the samples, we retrieve the principal hydraulic conductivities, k_1^s and k_2^s, and the angles, θ^s, that the x-axis of the butted sample makes with the direction of k_1^s for each sample. Then, in the final step, we can use either of the possible configurations to retrieve the contact surface position by employing pressure readings alone.

Starting with configuration 'XY', we prescribe six pressure measurements in the sample X at coordinate positions $(0.25,0)$, $(0.35,0)$, $(0.45,0)$ on the bottom no-flow face and $(0.25,1)$, $(0.35,1)$, $(0.45,1)$ on the top no-flow face. This information, coupled with the average flux at the inflow face $x=0$, produces highly accurate results for sample X, typical to those of Run1 in Tab. 2.

Table 2: Numerical results for the GA simultaneous recovery of the principal hydraulic conductivities, k_1^s and k_2^s, the angles, θ^s, and the contact surface position when the inversion is performed in steps.

	Run1		
Coefficient	Exact	Range	Results
k_1^X	5	$[4.5,5.5]$	4.99
k_2^X	1	$[0.5,1.5]$	1.00
θ^X	30°	$[20°,40°]$	29.98
k_1^Y	5	$[4.5,5.5]$	5.43
k_2^Y	1	$[0.5,1.5]$	0.80
θ^Y	60°	$[50°,70°]$	69.38
$x_b^f = x_t^f$	1.33	$[1.0,2.0]$	1.63

	Run2		
Coefficient	Exact	Range	Results
k_1^X	5	$[4.5,5.5]$	5.37
k_2^X	1	$[0.5,1.5]$	0.98
θ^X	30°	$[20°,40°]$	23.64
k_1^Y	5	$[4.5,5.5]$	4.99
k_2^Y	1	$[0.5,1.5]$	0.99
θ^Y	60°	$[50°,70°]$	60.03
$x_b^f = x_t^f$	0.67	$[0.5,1.5]$	0.86

Reversing the flow direction is equivalent to considering the configuration 'YX'. In that case, the same information is expected to provide good estimates for the principal hydraulic conductivities, k_1^Y and k_2^Y, and the angle, θ^Y, that the x-axis of the sample makes with the direction of k_1^Y, with results typical to those of Run2 in Tab. 2.

With the values of the unknown hydraulic conductivity parameters obtained accurately from the first two steps of the inversion, we then perform a final step in which we use only pressure information to determine the contact surface. For either of the configurations 'XY' or 'YX', and provided that we take pressure readings in both samples, the contact surface location can usually be obtained accurately. For example, when considering the configuration 'XY' and extra pressure readings on the bottom no-flow boundary at the coordinate positions $(0.35,0)$, $(1.65,0)$, a typical retrieved value for the position of the contact surface interface was $x_b^f = x_t^f = 1.33$. Although this three-step inversion technique very accurately estimates the hydraulic parameters, the relatively large number of additional measurement ports makes this approach expensive.

5.2 *Oblique contact surface: $x_t^f \neq x_b^f$ (case (b))*

For the more general case of the contact surface determined by the straight line d that joins the coordinate points $(x_b^f,0)$ and $(x_t^f,1)$, see Fig. 1, and provided that the principal hydraulic conductivities, k_1^s and k_2^s, and the angles, θ^s, are given, we reach a similar conclusion to the case when the contact surface was perpendicular to the x-axis of the butted sample, namely that pressure alone measured in both samples, either side of the contact surface, will ensure an accurate retrieval of the positions x_t^f and x_b^f. For example, if we take $x_t^f = 1.42$ and $x_b^f = 1.23$ and pressure readings at the coordinate positions $(0.35,0)$, $(1.65,0)$ on the bottom no-flow face and $(0.35,1)$, $(1.65,1)$ on the top no-flow face, we obtain very accurate estimates of the contact surface positions such as $x_b^f = 1.23$ and $x_t^f = 1.42$ for a domain of search $(x_b^f, x_t^f) \in \mathscr{D} = ([0.5,1.5]\times[0.5,1.5])$.

When applying the three-step inversion, we experimented with different numbers of measurement ports located along the no-flow boundaries of the upstream sample, namely sample X from the 'XY' configuration. Table 3 shows that increasing the number of ports improves the accuracy of k_1^X, k_2^X and θ^X. However, for a reasonable number of ports, we do not estimate these values as accurately for oblique contact surfaces as for perpendicular ones.

Table 3: Numerical results for the GA simultaneous recovery of the principal hydraulic conductivities, k_1^s and k_2^s, the angles, θ^s, and the contact surface position for different numbers of pressure measurement ports.

			Results		
Coefficient	Exact	Range	6 Ports	8 Ports	9 Ports
k_1^X	5	$[4.5, 5.5]$	5.19	5.08	5.05
k_2^X	1	$[0.5, 1.5]$	1.04	1.01	1.01
θ^X	30°	$[20°, 40°]$	31.29	30.47	30.28
k_1^Y	5	$[4.5, 5.5]$	4.58	4.79	5.05
k_2^Y	1	$[0.5, 1.5]$	1.03	1.11	1.06
θ^Y	60°	$[50°, 70°]$	58.22	61.43	61.88
x_b^f	1.23	$[1.0, 1.5]$	1.15	1.06	1.15
x_t^f	1.42	$[1.0, 1.5]$	1.39	1.44	1.46

The conclusion remains the same when we reverse the flow direction. For example, in the case of measurements from eight ports in sample Y, typical results of the inversion were no better than $\left(k_1^Y, k_2^Y, \theta^Y\right) = (4.92, 1.06, 59.71)$. With these values and the ones in Tab. 3 obtained for eight ports for sample X, the third step of the inversion, using only pressures, produced estimates of the contact surface positions such as $x_b^f = 1.19$ and $x_t^f = 1.45$, with relative approximation errors of 3.23% and 2.08%, respectively.

6 Comparison of inversion methods

In this section, by means of a comparison with the more traditional, gradient based, optimisation techniques, we perform a detailed comparative study that attempts to discuss the relevance of the genetic algorithm technique to the particular problem of identifying the components of the hydraulic conductivity tensors and the contact surface position in the case when it is perpendicular to the x-axis of the butted sample (case (a)). The information that we use in the inversion process combines the pressure recorded at ports on the bottom and top no-flow boundaries and the average inflow flux.

The traditional gradient method that we use is the derivative-based iterative NAG routine E04KCF, which performs a quasi-Newton algorithm for finding the minimum of a function of several variables, subject to simple bounds on the variables. In this case, the objective function which is minimised is $\text{LS}^{-1} - \alpha$, see Eq. (7). The gradient of this functional is calculated using forward differences.

The same type of additional information added into the GA inversion process was used by the NAG routine to perform the inversion. Based on the pressure measurement ports for which the GA performed a successful simultaneous retrieval of all the unknown parameters, namely in the fully specified situation when pressure measurements were recorded at the coordinate points $(0.35, 0)$, $(0.65, 0)$, $(1.55, 0)$, $(1.85, 0)$ on the bottom no-flow face and $(0.55, 1)$, $(1.75, 1)$ on the top no-flow face, we study the behaviour of the NAG optimisation procedure. We perform a sequence of experiments, starting with the underspecified situation, where we have one measurement port in each sample. We build up to the fully specified situation in which we measure pressure at all of the above points. The ranges for the NAG inversion, i.e. the simple bounds on the variables, were the same as for the GA (Run2 in Tab. 1). We used the average influx flow and the following data: pressure readings at (i) $(0.35, 0)$, $(1.55, 0)$; (ii) $(0.35, 0)$, $(1.55, 0)$, $(0.55, 1)$; (iii) $(0.35, 0)$, $(1.55, 0)$, $(1.75, 1)$; (iv) $(0.35, 0)$, $(1.55, 0)$, $(0.55, 1)$, $(1.75, 1)$; (v) $(0.35, 0)$, $(0.65, 0)$, $(1.55, 0)$, $(0.55, 1)$, $(1.75, 1)$; and the fully specified situation (vi) pressure readings at $(0.35, 0)$, $(0.65, 0)$, $(1.55, 0)$, $(1.85, 0)$, $(0.55, 1)$, $(1.75, 1)$. Table 4 shows the results of the NAG inversion when we used the same initial guesses for each numerical simulation. We observe that the estimation error decreases as we move towards the fully specified situation and the results are very accurate in the final situation.

Table 4: Numerical results of the inversion process when using the NAG routine and the information as described by cases (i)–(vi).

Value	Exact	Results (i)	(ii)	(iii)	(iv)	(v)	(vi)
k_1^X	5	4.50	4.50	4.50	5.50	5.01	5.00
k_2^X	1	0.76	0.83	0.80	1.13	1.00	1.00
θ^X	30°	20.00	23.36	24.01	34.61	30.07	30.00
k_1^Y	5	4.50	4.50	4.50	4.50	4.50	5.00
k_2^Y	1	0.97	0.86	0.99	0.98	0.98	1.00
θ^Y	60°	57.73	50.00	58.30	58.20	58.25	60.00
$x_b^f = x_t^f$	1.33	1.19	1.13	1.29	1.35	1.32	1.33

For an underspecified situation the results are not optimal but do provide a very good match to the measured data. This is due to the non-uniqueness that the underspecification produces, a situation which was also encountered in the case of the GA optimisation. However, in such cases, in order to produce better results, we can provide good initial guesses for the NAG routine using results from the GA optimisation. Then, despite the underspecification of the situation, it is possible to achieve results close to their optimal values.

Table 5 shows results from using the GA procedure outputs as initial guesses for the NAG routine. Numerical results are presented for the underspecified case (v) and using various initial guesses for the NAG algorithm. It is observed that in the cases of Run1 and Run2, where reasonably good initial guesses are imposed, the algorithm however fails to render accurate results, whereas in Run3, where the initial guesses are given by the GA, the NAG optimisation produces close to optimal results.

If we consider now the fully specified situation encountered in the three-step inversion technique of Section 5.1, namely we consider that six pressure readings are available in the first sample, then, unless a close to optimal initial guess is prescribed, the NAG routine does not provide the optimal, or close to the optimal, solution. This is due to the fact that such a situation implies a degree of underspecification for the second sample. For example, in ranges of search such as the ones prescribed for the GA, namely

Table 5: Numerical results of the NAG inversion for the case (v) and different initial guesses for the parameters.

Value	Exact	Run1 Guess	Run1 Results	Run2 Guess	Run2 Results
k_1^X	5	4.75	5.50	4.95	5.13
k_2^X	1	1.20	1.13	0.95	1.04
θ^X	30°	27.0	34.61	29.0	31.35
k_1^Y	5	5.20	4.50	4.95	4.50
k_2^Y	1	0.75	0.98	0.95	0.99
θ^Y	60°	62.0	58.14	59.0	58.19
$x_b^f = x_t^f$	1.33	1.21	1.35	1.31	1.33

Value	Exact	Run3 Guess	Run3 Results
k_1^X	5	5.19	4.95
k_2^X	1	1.04	0.98
θ^X	30°	31.02	29.46
k_1^Y	5	4.77	5.00
k_2^Y	1	1.00	1.00
θ^Y	60°	59.06	60.02
$x_b^f = x_t^f$	1.33	1.33	1.33

from Run1 of Tab. 2, a good initial guess such as $\left(k_1^X, k_2^X, \theta^X\right) = (5.25, 0.75, 28.0)$, $\left(k_1^Y, k_2^Y, \theta^Y\right) = (4.75, 0.65, 66.0)$ and $x_b^f = x_t^f = 1.31$ produces good estimates for the principal hydraulic conductivities of only the first sample, k_1^X and k_2^X, and the angle, θ^X, of the form $\left(k_1^X, k_2^X, \theta^X\right) = (5.00, 1.00, 30.00)$. However, a poor initial guess such as $\left(k_1^X, k_2^X, \theta^X\right) = (4.6, 0.6, 21.0)$, $\left(k_1^Y, k_2^Y, \theta^Y\right) = (5.4, 0.4, 51.0)$ and $x_b^f = x_t^f = 1.51$ produces inaccurate results within the first sample, such as $\left(k_1^X, k_2^X, \theta^X\right) = (4.50, 0.70, 20.00)$, as well as in the second sample. This situation is not encountered by the GA optimisation, which combines effectively the information in the same domain of search to produce close to optimal solutions for the hydraulic parameters in the first sample. Similar conclusions can be drawn with respect to the retrieval of the hydraulic properties of the second sample by reversing the flow direction. Then, following the third step in this inversion procedure, we have an overspecified situation for determining the contact surface location. Provided that good initial guesses are used in the first two steps of the inversion, thus ensuring good estimates of the hydraulic parameters for both samples, the contact surface location can usually be determined with high accuracy, as in the case of the GA inversion.

7 Conclusions

In this paper we have dealt with the identification of the hydraulic conductivity tensors and the contact surface location for a composite anisotropic material. The success of the GA retrieval depends on the degree of specification of the unknowns. Whilst in an underspecified situation the GA fails to render accurate results, when sufficient information is prescribed the GA produces stable and accurate results. The GA also deals with the situation when just one of the sets of parameters describing the components of the hydraulic properties of one of the samples is fully specified or overspecified, in which case the inversion can be performed in steps by means of reversing the direction of the flow through the butted sample. In a fully specified situation, a traditional NAG optimisation technique behaves, for this particular problem, better than the GA optimisation. However, whenever some degree of underspecification is encountered the GA usually produces better results. A method of producing good results when an underspecified and realistic situation is encountered, namely with a reduced number of ports, is to combine the GA with the NAG optimisation technique, where the GA is applied initially to provide a good initial guess for the NAG algorithm. Although noise in the measurement data has not been considered in this paper, from previous studies [Mustata, Harris, Elliott, Ingham, and Lesnic (1999); Mustata, Harris, Elliott, Lesnic, Ingham, Khachfe, and Jarny (2001)] we believe that accurate results for the type of inverse problem studied here will still be achieved in such situations.

References

Bernabe, Y. (1992): On the measurement of permeability in anisotropic rocks. In Evans, B.; Wong, T.-F.(Eds): *Fault mechanics and transport properties of rocks*, pp. 147–167. Academic Press, London.

Brebbia, C. A.; Telles, J. C. F.; Wrobel, L. C. (1984): *Boundary element techniques: Theory and application in engineering*. Springer-Verlag, Berlin.

Durlofsky, L. J.; Chung, E. Y. (1987): Effective permeability of heterogeneous reservoir regions. In *Second European conference on the mathematics of oil recovery*, pp. 57–64. Editions Techniq, Paris.

Fontugne, D. J. (1969): *Permeability measurement in anisotropic media*. PhD thesis, Syracuse University, Syracuse, NY, 1969.

Huang, C.-H.; Shih, C.-C. (2007): An inverse problem in estimating simultaneously the time-dependent applied force and moment of an Euler–Bernoulli beam. *CMES: Computer Modeling in Engineering and Sciences*, vol. 21, pp. 239–254.

Ling, X.; Atluri, S. N. (2006): Stability analysis for inverse heat conduction problems. *CMES: Computer Modeling in Engineering and Sciences*, vol. 13, pp. 219–228.

Liu, C.-S. (2006): An efficient simultaneous estimation of temperature-dependent thermophysical properties. *CMES: Computer Modeling in Engineering and Sciences*, vol. 14, pp. 77–90.

Liu, C.-S.; Liu, L.-W.; Hong, H.-K. (2007): Highly accurate computation of spatial-dependent heat conductivity and heat capacity in inverse thermal problem. *CMES: Computer Modeling in Engineering and Sciences*, vol. 17, pp. 1–18.

Marin, L.; Power, H.; Bowtell, R. W.; Sanchez, C. C.; Becker, A. A.; Glover, P.; Jones, A. (2008): Boundary element method for an inverse problem in magnetic resonance imaging gradient coils. *CMES: Computer Modeling in Engineering and Sciences*, vol. 23, pp. 149–174.

Mei, C. C.; Auriault, J.-L. (1989): Mechanics of heterogeneous porous media with several spatial scales. *Proceedings of the Royal Society of London*, vol. A426, pp. 391–423.

Mera, N. S.; Elliott, L.; Ingham, D. B. (2006): The detection of super-elliptical inclusions in infrared computerised axial tomography. *CMES: Computer Modeling in Engineering and Sciences*, vol. 15, pp. 107–114.

Mustata, R.; Harris, S. D.; Elliott, L.; Ingham, D. B.; Lesnic, D. (1999): Parameter identification in a boundary element model of a hydraulic pump flow test. In Aliabadi, M. H.(Ed): *Proceedings of the first international conference on boundary element techniques*, pp. 331–340. Queen Mary & Westfield College, University of London.

Mustata, R.; Harris, S. D.; Elliott, L.; Lesnic, D.; Ingham, D. B.; Khachfe, R. A.; Jarny, Y. (2001): The determination of the properties of orthotropic heat conductors. In Petit, D.; Ingham, D. B.; Jarny, Y.; Plourde, F.(Eds): *Inverse problems and experimental design in thermal and mechanical engineering*, pp. 325–332. Proceedings of the Eurotherm seminar 68, 5–7 March, 2001, Poitiers, France.

Rose, W. D. (1970): New method to measure directional permeability. *Journal of Petroleum Technology*, vol. 34, pp. 1142–1144.

Saez, A. E.; Otero, C. J.; Rusinek, I. (1989): The effective homogeneous behaviour of heterogeneous porous media. *Transport in Porous Media*, vol. 4, pp. 213–238.

Shiozawa, D.; Kubo, S.; Sakagami, T.; Takagi, M. (2006): Passive electric potential CT method using piezoelectric material for identification of plural cracks. *CMES: Computer Modeling in Engineering and Sciences*, vol. 11, pp. 27–36.

White, C. D.; Horne, R. N. (1987): Computing absolute transmissibility in the presence of fine-scale heterogeneity. In *Symposium on reservoir simulation*, San Antonio, TX, SPE Paper 16001.

Zhan, L.; Yortsos, Y. C. (2001): A direct method for the identification of the permeability field of an anisotropic porous medium. *Water Resources Research*, vol. 37, pp. 1929–1938.